

# Novel Process Method to Prepare Yttria Stabilized ZrO<sub>2</sub> Beads Based on the Sol-Gel Titration Technology

Xiaodong Wang<sup>a\*</sup> , Yunfeng Qin<sup>a</sup>, Ang Zhang<sup>a</sup>, Hui Han<sup>a</sup>, Yonghe Wang<sup>a</sup>

<sup>a</sup>Anhui Triumph Applied Materials Co., LTD., Bengbu, China.

Received: December 5, 2024; Revised: March 3, 2025; Accepted: March 23, 2025

Based on the sol-gel titration technology, a novel process method to prepare the ZrO<sub>2</sub> beads with the advantages of 130 nm grains and no pores is proposed. These advantages can greatly improve the bead density and hardness, decline the sintering temperature. Furthermore, the proposed method can prepare different types of the beads whose diameters range from 0.1 mm to 0.8 mm, and with uniform size and well spherical type. The density of the bead tested results mainly concentrate on 6.04 g/cm<sup>3</sup>, and the hardness on 1280 HV. The SEM investigation results illustrate that the bead grains are evenly distributed. The surface and cross section of the bead grains are consistent, no pores exist among the grains of finely polished section. The XRD tested results demonstrate that no monoclinic phase exists in the bead. The bead sintering temperature is only 1250 °C.

**Keywords:** *Small grains, Low sintered temperature, Sol-gel titration technology, Different diameters yttria stabilized ZrO<sub>2</sub> beads.*

## 1. Introduction

Due to the excellent characteristics of high hardness, high wear resistance, high corrosion resistance, large bulk density and high grinding efficiency, yttria stabilized ZrO<sub>2</sub> grinding beads are widely used in the grinding of oxidation ceramic powders<sup>1,2</sup>. In addition, they are also widely used in other fields<sup>3-7</sup>. With so many advantages and applications of the yttria stabilized ZrO<sub>2</sub> beads, they have been widely researched in these years.

In the previous reports, the main methods to prepare the yttria stabilized ZrO<sub>2</sub> beads were extrusion forming method, isostatic pressing forming method, rolling forming method, sol-gel method, and gelcasting method, etc. Jia et al.<sup>8</sup> prepared the ZrO<sub>2</sub> beads by dry cold isostatic pressing forming method under the molding pressure of 0.1 ~ 0.16 G Pa. But the experimental results showed that the wear resistance of the beads was bad. Lv<sup>9</sup> successfully accomplished ZrO<sub>2</sub> grinding medium beads by the rolling forming method, which the prepared bead density was only 5.92 g/cm<sup>3</sup> and the diameter was 2.7 mm. The rolling forming method has the advantages of simple process and large output, which has been widely applied to prepare the beads. But it is difficult to prepare the products with low wear resistance, which limits its application on high-end fields. Walter et al.<sup>10</sup> prepared the yttria stabilized ZrO<sub>2</sub> beads by gel method for supported precipitation. But the sintering temperature of the method was 1600 °C. Lv et al.<sup>9</sup> prepared 0.2 - 0.3 mm yttria stabilized ZrO<sub>2</sub> beads by gelcasting method. But the monoclinic phase also existed when the beads were sintered at 1525 °C.

The sol-gel titration technology is based on the sol-gel method, and combined with titration process. Guo et al.<sup>11</sup> supplied the ZrO<sub>2</sub>-Al<sub>2</sub>O<sub>3</sub> composite beads by internal gelation method, and studied the effects of Al<sup>3+</sup> on the stability of

the solution and its performance of gel spheres. Liu et al.<sup>12</sup> prepared the Al<sub>2</sub>O<sub>3</sub> beads by this technology which were used for catalyst support. However, up to now, there is no research on the preparation of yttria stabilized ZrO<sub>2</sub> beads by this technology.

In this report, based on the sol-gel titration technology, an innovative method to prepare the yttria stabilized ZrO<sub>2</sub> beads is proposed, which can prepare the ZrO<sub>2</sub> beads with the advantages of 130 nm grains and no pores. These advantages can greatly improve the density and hardness of the beads, and obviously decline the sintering temperature. Furthermore, using the method, the beads of different diameters which range from 0.1 mm to 0.8 mm can be prepared, and the beads can be controlled with the uniform size and well spherical type. To illustrate the novel method, the beads whose diameters were 0.1 mm, 0.2 mm, 0.3 mm, and 0.5 mm were prepared and studied. They were prepared by the sol-gel preparation, titration process, organic compound discharging and sintering steps. In the titration step, the titration beads with different diameters were mainly dominated by controlling the viscosity and specific gravity of sol, selecting different sizes of titrating needle type. The results show that the prepared beads have uniform size and well spherical type. The Morphology tests were made after the beads titrated, baked at 120 °C, glue discharged at 550 °C and sintered at 1250 °C. The results show that the beads are bright, which indicates that the surface of beads is smooth, and have few defects. The bead samples were characterized by Archimedes drainage method and Vickers hardness test. The density tested results mainly concentrate on 6.04 g/cm<sup>3</sup>, and the hardness on 1280 HV. Both of the them are higher than that of the previous beads prepared by the conventional methods. The surface and internal grains of the beads were also characterized by SEM, and their micro-

\*e-mail: wangxiaodong8530@126.com

morphologies were obtained. The results show that the grains are evenly distributed. The tested average grain size is 130 nm, much smaller than 400 nm that of beads prepared by the conventional process. Moreover, the surface and cross section of the bead grains are consistent, and no pores exist among the grains of finely polished section. The XRD tested results demonstrate that no monoclinic phase exist in the bead. Furthermore, the bead sintering temperature of the new proposed process method is only 1250 °C, much lower than the routine methods.

The rest of the report is organized as follows: In section II, we first propose the used materials in experiments and the process steps of the novel method. Then, the experiments to illustrate the new method are shown. Finally, the influences of the preparation conditions are discussed. In section III, the prepared bead density, hardness, morphology, crystal phase characterizations and related discussions are made. In section IV, we give a brief conclusion.

## 2. The Process Steps, Experiments and Discussions

### 2.1. Materials and Methods

#### 2.1.1. Chemicals

The used raw materials in experiments included  $\text{ZrOCl}_2 \cdot 8\text{H}_2\text{O}$  (AR, Sinopharm Chemical Reagent Co., Ltd, 99.5%),  $\text{YCl}_3$  (AR, Sinopharm Chemical Reagent Co., Ltd, 99.99%), ammonium hydroxide (AR, Sinopharm Chemical Reagent Co., Ltd, 25%), PVA 205 (AR, Japanese Kola Li Co., Ltd, 15%), tetrahydrofurfuryl alcohol (AR, Sinopharm Chemical Reagent Co., Ltd, 98%), acetic acid (AR, Sinopharm Chemical Reagent Co., Ltd, 99.8%), deionized water, etc.

#### 2.1.2. The process steps

In the new process method, the detail steps to prepare the yttria stabilized  $\text{ZrO}_2$  beads are as follows:

##### Step 1: Prepare the solution

The zirconium oxychloride and yttrium chloride are dissolved in deionized water and mixed in the desired proportion. Here we use mechanical stirring method. The molar ratio of zirconium oxychloride to yttrium chloride and deionized water is 1:0.06:70. The ratio of the two substances is determined by the mass percentage of yttrium oxide in the yttria stabilized  $\text{ZrO}_2$  beads, the percentage is about 5 - 5.5%. The prepared sample was tested using X-ray fluorescence analysis, and the mass proportion of yttrium oxide was 5.205%.

##### Step 2: Add the ammonia

Add ammonia into the solution prepared in step 1 with mechanical stirring condition. The mass percentage of ammonia used in this step should be 5 - 7% which the pH is about 11.2. The ammonia must be added slowly, and the velocity should be about 20 ml/min. When the pH reaches to 1.5 - 2, stop adding ammonia, add acetic acid. The concentration of acetic acid is 99.8%, and acetic acid is directly poured into the solution. The weight of acetic acid should be 1% of the zirconium oxychloride. Continue stirring for 30 min, then continue adding ammonia. The final pH of the solution should

be up to 8.5 - 9. Then stop stirring and wait 30 minutes for the solution to stabilize.

##### Step 3: Remove the chloride ion

Handle the solution prepared in step 2 with filter-press method. The solution is a suspension, and the particle size test result using the particle size tester is  $D_{10}=2.5\mu\text{m}$ ,  $D_{50}=5.5\mu\text{m}$ ,  $D_{90}=16.3\mu\text{m}$ . The mesh size of the filter cloth of the filter press is 5000 mesh, which can collect solid particles. Then mix the sediment with deionized water, and well stir. To fully remove the chloride ion, this step should be repeated by 3 - 4 times. The water collected after each filtration is also clear and transparent.

##### Step 4: Dissolve the sediment

Prepare the mixed solution which dissolve zirconium oxychloride and yttrium chloride in deionized water, and the molar ratio of zirconium oxychloride to yttrium chloride and deionized water is 1:0.06:70, and heat to 70 - 80 °C. The added weight of zirconium oxychloride, yttrium chloride and deionized water is half of step 1. Then place the sediment (prepared in step 3) into the solution gradually with mechanical stirring condition, the sediment is added in stages, with about 20% of the weight added each time, and continue to be added after complete dissolution. The sediment can not be completely dissolved at room temperature, so the solution should be heated to 70 - 80 °C. The pH index of the solution should be monitored, the final pH should be controlled to 1.5 - 2. In acidic environment, the sediment in step 3 can be dissolved to form transparent solution. The solution is strongly acidic, and zirconium exists in the form of ions in the solution. The clarified solution can ensure that no large particles exist in solution and the titrated beads are nearly transparent.

For the beads of different diameters, the solution should be matched with different viscosity and specific gravity. Therefore, the viscosity and specific gravity of the solution need to be monitored and adjusted in this step. 1) For the bead diameters of 0.1 mm, the viscosity should be as low as possible, because the inner diameter of the discharging needle is very small, that is 0.24 mm. The viscosity should be  $1.2 - 1.5 \times 10^{-3} \text{ Pa} \cdot \text{s}$ . The specific gravity should be 1.05 - 1.08. 2) For the bead diameters of 0.2 - 0.3 mm, The viscosity should be  $20 - 25 \times 10^{-3} \text{ Pa} \cdot \text{s}$ , and the specific gravity should be 1.15 - 1.18. 3) For the bead diameters of 0.5 - 0.65 mm, the viscosity should be  $25 - 30 \times 10^{-3} \text{ Pa} \cdot \text{s}$ , and the specific gravity should be 1.20 - 1.25.

##### Step 5: Polymeric Binder Addition

Add PVA 205 (the solution with a solid content of 15%) and tetrahydrofurfuryl alcohol into the solution (prepared in step 4), stir the mixture to fully combine. The added weight of PVA 205 and tetrahydrofurfuryl alcohol should be about 2% and 1% than that of the solution prepared in step 4, respectively.

##### Step 6: Stepwise Addition and Bead Formation

The schematic diagram of titration equipment is shown in Figure 1. Place the solution (prepared in step 5) into solution tank, under the action of compressed air, the sol enters into the tank under the vibrator through the regulating valve. Then the sol drops into aqueous ammonium (The mass percentage of aqueous ammonium used here should be about 10% which the pH is about 11.8). Before dropping,

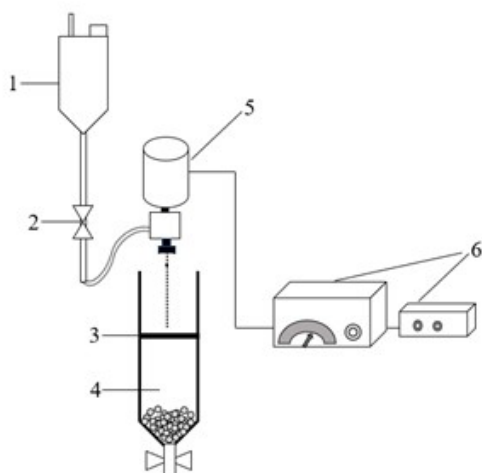


**Figure 1.** The schematic diagram of titrated equipment (1. solution tank. 2. regulating valve. 3. 8-Alkanes. 4. ammonia. 5. vibrator. 6. power source and regulator).

**Table 1.** The relationship of the bead size, the needle type, the viscosity and specific gravity of the solution.

The diameters of bead Samples	Viscosity (Pa·s)	Specific gravity	Needle model (G)
0.1 mm	$1.2-1.5 \times 10^{-3}$	1.05-1.08	26
0.2 mm	$20-25 \times 10^{-3}$	1.15-1.18	23
0.3 mm			21
0.5 mm	$25-30 \times 10^{-3}$	1.20-1.25	19
0.65 mm			16

the 8-Alkanes should be added into the ammonia to prevent ammonia volatilization, about 2 mm on the surface of ammonia. The 8-alkanes are isomeric alkanes, colorless and transparent liquids with a slight petroleum odor, and the density is 0.78 g/ml. The density of 8-Alkanes is lower than that of aqueous ammonium, so it can float on top of aqueous ammonium. To titrate different sizes of the beads, The corresponding type of titrated needle should be used. The solution comes out of the needle and under the action of a vibrator (providing positive rotation waves), the liquid column can be divided into small droplets, which form small beads under the action of surface tension. After buffering with 8-Alkanes, liquid drops solidify into small beads of zirconium hydroxide in aqueous ammonium. The experimental process can be carried out at room temperature without the need for temperature treatment of the solution. Generally, a temperature of 20-28°C is the most suitable. The relationships of the bead size, the viscosity and specific gravity of the solution, and the needle type are shown in Table 1. Different types of needles are shown in the Figure 2. The titration method used here is based on the surface tension to form the beads. Using this technology, the bead sizes of 0.1 - 0.8 mm can be prepared. In this report, our works mainly focus on the beads whose diameters are 0.1 mm, 0.2 mm, 0.3 mm and 0.5 mm.

#### Step 7: Clean the beads

Place the titrated beads into a Teflon grinding can and add an ammonia solution with 10% mass concentration. Then



**Figure 2.** The different types of discharging needle.

place the can into the planetary mill and rotate at 100–150 RPM. The pH of the ammonia solution is about 11.8. The ratio of the volume of ammonia solution to the volume of the beads here is approximately 5:1. The rotation of the tank drives the beads move, and achieves to the purpose of chloride ion precipitation. This step needs to be repeated by 3 - 4 times to ensure that the content of chloride ion below 100 ppm. If the content of chloride ion too high, the chloride ion will be discharged during the sintered process, which will affect the compactness of the beads.

#### Step 8: Bake the beads

Place the beads (prepared in step 7) into oven and bake. The temperature of the oven should be about 120 °C. The beads need to be baked in the crucible. The crucible must be covered tightly. The detail discussions on the Influence of baking conditions are shown in section 2.2.1.

#### Step 9: Thermal Debinding

Place the beads (prepared in step 8) into debinding furnace and discharge. The rising time-temperature curve of debinding furnace should be: 2 hours rise to 160 °C, keep the temperature for 1 hour, 25 hours rise to 550 °C, and keep the temperature for 2 hours.

#### Step 10: Sinter the beads

Place the beads (prepared in step 9) into sintering furnace. The sintering step do not need any special isolation. The sintering rising-time temperature curve has great influence on the grain of the beads. Abnormal sintering rising-time temperature curve will lead to the defects and pores among grains emergence, or abnormal grains growth. The detail discussions on the influence of the sintering rising-time temperature curve to beads are shown in section 2.2.2. The final sintering rising-time temperature curve we selected is: 11 hours rise to 1250 °C (no insulation), and naturally cool to room temperature.

## 2.2. Beads sample preparation

Using the new process method, the ZrO<sub>2</sub> bead samples whose diameters were 0.1 mm, 0.2 mm, 0.3 mm, 0.5 mm were prepared. to simplify the subsequent statements, they

are marked as 0.1 mm beads, 0.2 mm beads 0.3 mm beads and 0.5 mm beads, respectively.

In order to exhibit the beads of different states when processing. The beads after titrated, baked at 120 °C, removal of the organic binder at 550 °C and sintered at 1250 °C are shown. To illustrate the uniformity and sphericity of the beads, the morphologies of 0.1 mm beads and 0.3 mm beads under optical microscope are also shown.

### 2.2.1. The beads of different states after titration

Figure 3 show the beads of different states. 1) After the titrating step: as can be seen from Figure 3a, the beads after titrated are nearly transparent, which are related to the transparency of the configured sol. In this stage, the titrated beads are very soft and can not be exerted by large force. 2) After baking step at 120 °C: the beads after baked in the crucible are brownish yellow which are shown in Figure 3b, because there are organic matters in the sol which change the beads colour when baked. The baked beads are very bright, which are relevant with the smooth surface of the beads. In this process, the beads shrink, and the baked beads have relatively high strength. 3) After glue discharging step at 550 °C: the beads are similar to glass and nearly transparent, as shown in Figure 3c, which implies that the interior of the beads is dense without pores and defects. 4) After sintering step at 1250 °C: the sintered beads are very bright, as shown in Figure 3d, which implies that the surface of the beads prepared by the new process is very smooth. Using the new

process method, the polished process does not need. However, the surface of the beads prepared by rolling method is rough. They need to be polished to achieve bright<sup>13</sup>.

### 2.2.2. Morphologies of the sintered beads under Optical microscope

To illustrate the smoothness, uniformity and sphericity of the beads after sintering step, the morphologies of 0.1 mm beads and 0.3 mm beads under optical microscope are shown. The used optical microscope tests equipment was double tube microscope, as shown in Figure 4a. The tested results of 0.1 mm beads and 0.3 mm beads are shown in Figures 4b and 4c, respectively. From Figures 4b and 4c, it can be seen that the beads are bright, have uniform size and well spherical type.

### 2.3. Preparation conditions discussion

#### 2.3.1. The influence of baked conditions on beads

The beads after titrating step are mainly composed of zirconium hydroxide, bound water and organic matters. The speed of water evaporation must be controlled slowly in baking step. The baked conditions of wet beads should be slowly completed under conditions of high relative humidity. Otherwise, there is risk that the surface of the wet beads will preferentially dehydrate and seal the channels of water molecules, resulting in shiny drying beads with

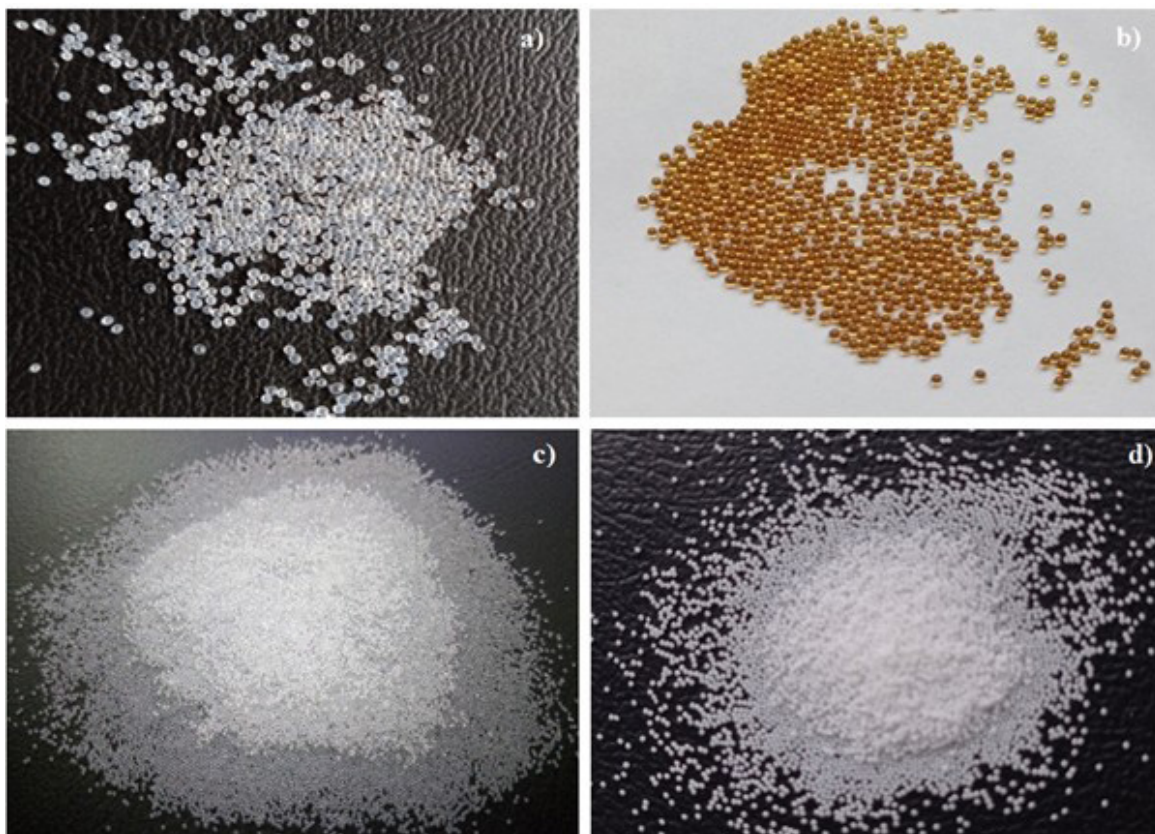


**Figure 3.** The different states of the beads in processing: (a) After titrating step. (b) After baking step at 120 °C. (c) After glue discharging step at 550 °C. (d) After sintering step at 1250 °C.

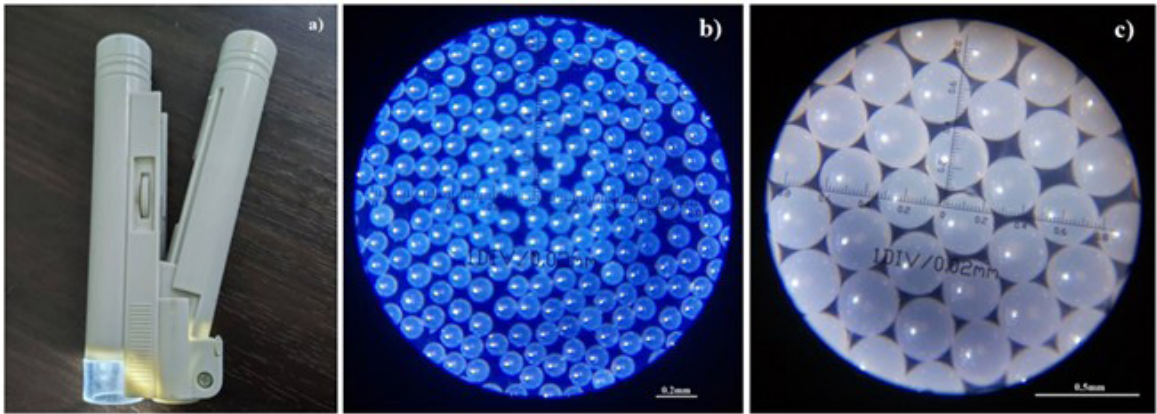


**Figure 4.** (a) The double tube microscope. (b) The morphology of 0.1 mm beads after sintered at 1250 °C under optical microscope. (c) The morphology of 0.3 mm beads after sintered at 1250 °C under optical microscope.

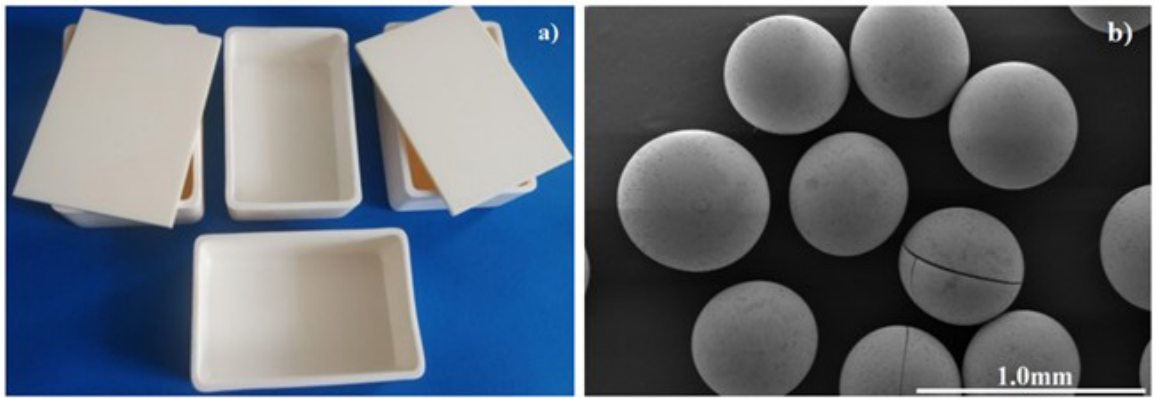


**Figure 5.** (a) The crucibles used in experiments. (b) The SEM images of cracking beads after sintering step when the crucible without lid in baking step.

ineffective release of internal moisture. Baking method for lid cover can increase the relative humidity inside, achieving synchronous dehydration of the beads surface and interior. Hence, the baking step must be carried out in the crucible with lid. And the crucible must be covered tightly. The used crucibles in experiments are shown in Figure 5a. To make comparison, the beads baked in the crucible without lid were prepared, the beads can not see any abnormal phenomenon after baked. However, after sintered, it can be seen by SEM that many cracking beads appear, as shown in Figure 5b. We conducted a comparative experiment on the methods of lid baking and open baking. The beads baked with lids had no cracking after sintering, while the beads baked with open lids had a cracking rate of about 36% after sintering.

### 2.3.2. The influence of sintering rising-time temperature curve on beads

The sintering rising-time temperature curve has great influence on the grain growth and distribution of the beads. To make comparison, three abnormal sintering rising-time temperature curves were used to sinter the 0.3 mm beads. The abnormal sintering rising-time temperature curve 1 (abbreviated as ASRTC 1 in subsequent sections) was: 11 hours rose to 1100 °C (no insulation), and naturally cooled to

room temperature. Abnormal sintering rising-time temperature curve 2 (abbreviated as ASRTC 2 in subsequent sections): 11 hours rose to 1200 °C (no insulation), and naturally cooled to room temperature. Abnormal sintering rising-time temperature curve 3 (abbreviated as ASRTC 3 in subsequent sections): 11 hours rose to 1300 °C, heated preservation for 3h, and naturally cooled to room temperature.

For the ASRTC1, the result is shown in Figure 6a. It can be seen that there are many pores among the grains on the surface of bead. The reason is that the grains grow incompletely in the sintering step. The existence of pores will reduce the compactness of the bead, and cause the decreasing of the bead density and wear resistance.

For the ASRTC 2, the result is shown in Figure 6b. It can be seen that when the temperature rises to 1200 °C, the pores among grains are significantly reduced, but a small amount of pores still exist, which indicates that the sintering temperature still need to be increased.

For the ASRTC 3, the result is shown in Figure 6c. It can be seen that there are many abnormal grains grown on the surface of bead. The reason is that the sintering temperature is too high and there is 3 hours preservation at 1300 °C. The abnormal grains growth can reduce the hardness of bead and decrease the wear resistance of bead.

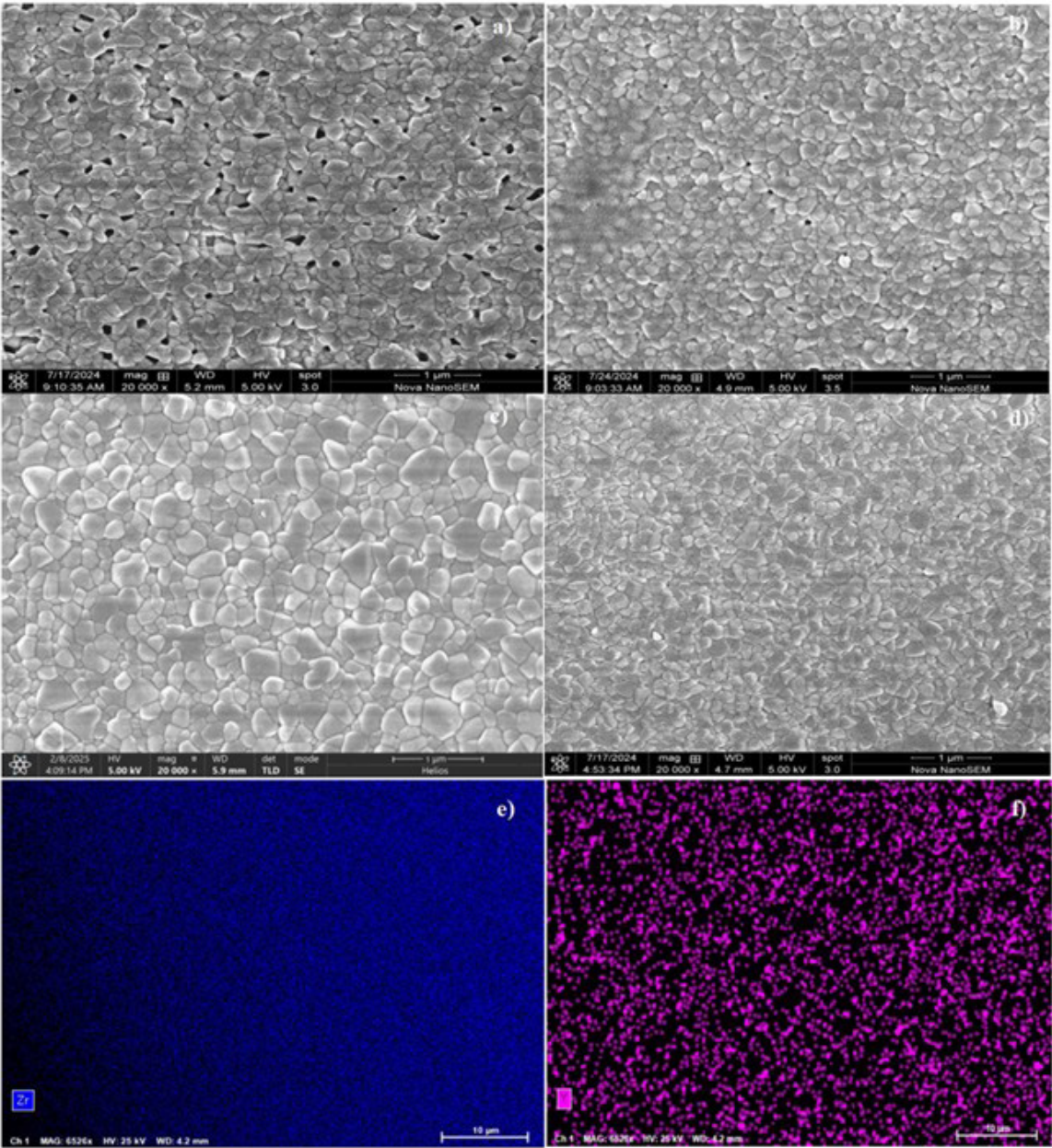


**Figure 6.** The SEM images of the surface morphology of 0.3 mm beads: (a) The surface grains morphology of the beads when the ASRTC1 was used. (b) The surface grains morphology of the beads when the ASRTC2 was used. (c) The surface grains morphology of the beads when the ASRTC3 was used. (d) The surface grains morphology of the beads when the normal sintering temperature curve was used. EDS analysis: (e) elemental Zr, (f) elemental Y.

The beads with normal grains and no pores can be obtained according to the sintering rising-time temperature curve proposed in section 2.1.2 step 10, and the result is shown in Figure 6d. Through the experiment of three curves, we can see that the heating rate, holding temperature, and time have a significant impact on the grain size of the sintered sample. It is necessary to explore the appropriate heating rate, insulation temperature, and time for the sample formula based on the condition of the furnace. The obtained samples can be tested by SEM through experiments to obtain the size

and morphology of the grains, and then the heating rate, holding temperature, and time can be optimized. Finally, the optimal sintering parameters were obtained.

The sintering temperature of the beads prepared by the new sol-gel titration technology is only 1250 °C, and without insulation. However, in the traditional rolling process, the sintering temperature is generally above 1500 °C<sup>1,8,9,14,15</sup>, which further reflects the advantage of the new sol-gel titration technology. The EDS analysis results which shown in Figures 6e and 6f show that zirconium and yttrium elements are evenly distributed.

## 2.4. Sample testing conditions

### 2.4.1. Vickers hardness

For yttria stabilized ZrO<sub>2</sub> beads, the hardness characteristics is an important index. In this report, using the JMHVS-10-xyz automatic precision Vickers hardness tester, the hardness of 0.2 mm beads, 0.3 mm beads, and 0.5 mm beads were tested. The 0.1 mm beads is too small, and can not to be tested by the used equipment. Thus, it is not discussed here. To make comparison, the rolling forming beads whose diameter was 0.3 mm were also tested. All samples were tested in the force of 9.8 N.

### 2.4.2. SEM tests

The SEM were used to characterize the bead samples, and the used equipment was JSM-6510A (JEOL). Stick the sample beads onto the conductive tape, and place the sample in the coating machine, and spray the sample with gold for 40 seconds.

### 2.4.3. XRD analysis

The samples were analyzed by X-ray diffractometer (D 8, Siemens), Cu-K $\alpha$  ray, 40 kV, 40 mA, 2 $\theta$  range of 10°-85°, scanning speed 4°/min.

## 3. Characterization and Discussion of Experimental Results

### 3.1. Density

The used density test method was the Archimedes drainage method, and four bead samples were tested. The results are shown in Table 2. The main discussions are as follows: 1) The density tested results are in the scope of 6.01 - 6.06 g/cm<sup>3</sup>, concentrate on 6.04 g/cm<sup>3</sup>, which are very close to the theoretical density of 6.05 g/cm<sup>3</sup>. However, the tested results of the bead density prepared by the traditional rolling process were generally less than 6.0 g/cm<sup>3</sup><sup>9,14,15</sup>. This implies that the new sol-gel titration technology has advantages to prepare the beads with more compact grains, containing no pores, and few defects. The SEM results of 3.3.1 also show that the prepared beads contain few obvious defects and pores among the grains on the surface and interior of the beads. No pores and defects are conducive to the improvement of the bead hardness and wear resistance. 2) It can be seen from Figures 6a and 6b that the 0.3 mm beads prepared with the abnormal sintering rising-time temperature curves will cause the pores and defects among the grains. The tested density of the bead sample sintered by the ASRTC 1 is only 5.99 g/cm<sup>3</sup>, and the bead sample sintered by the ASRTC2 is 6.01 g/cm<sup>3</sup>. Both of them are smaller than that of beads prepared with the normal sintering rising-time temperature curve.

### 3.2. Vickers hardness

The test method steps were: 1) The sample beads were embedded in an epoxy resin. 2) After inlaying and curing, the sample block was ground with grinding and polishing equipment to expose the flat cross section of the beads which was shown in Figure 7. 3) Put the sample block into the hardness tester for testing. Each sample was tested by five times.

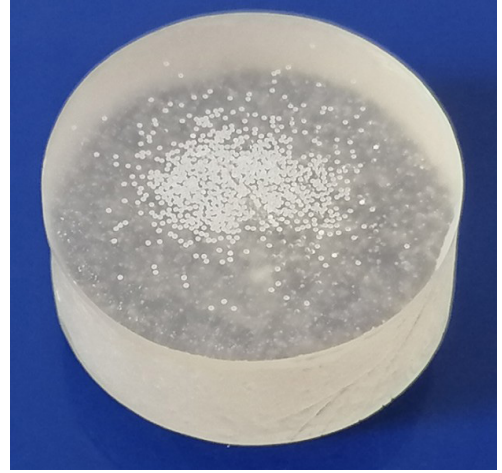


Figure 7. Sample block for hardness test.

Table 2. The densities of the 0.1 mm, 0.2 mm, 0.3 mm, and 0.5 mm bead samples sintered with the normal sintering rising-time temperature curve. For each sample, five group tests were made.

Number	Sample	0.1 mm beads	0.2 mm beads	0.3 mm beads	0.5 mm beads
1	Density (g/cm <sup>3</sup> )	6.03	6.01	6.01	6.02
2		6.04	6.03	6.03	6.02
3		6.04	6.05	6.04	6.05
4		6.05	6.05	6.05	6.06
5		6.06	6.05	6.06	6.06
Average value (g/cm <sup>3</sup> )		6.044	6.038	6.038	6.042

Table 3. The hardness of 0.2 mm, 0.3 mm and 0.5 mm bead samples sintered with the normal sintering rising-time temperature curve. For each sample, five group tests were made.

Number	Sample	0.2mm beads	0.3mm beads	0.5mm beads	Rolling forming beads of 0.3mm
1	Vickers hardness (HV 0.98)	1256	1249	1233	1102
2		1266	1270	1280	1121
3		1288	1291	1291	1136
4		1289	1296	1299	1167
5		1301	1333	1312	1186
Average value (HV)		1280	1288	1283	1142

The results are shown in Table 3. From the results, it can be got that: 1) The hardness tested results are in the scope of 1250 - 1350 HV, concentrate on 1280 HV, have good consistency, and larger than 1142 HV that of beads prepared by the rolling forming beads. The results show that the new sol-gel titration process method has great improvement on the hardness of beads, about 12% lift-up. 2) The matching of sintering rising-time temperature curve has great influence on the hardness of beads. If the sintering temperature too low to the normal value, the grains will not completely grow, and there will be many defects and pores among the grains, as shown in Figures 6a and 6b. The defects and pores will cause the decline of the bead hardness. The average hardness tested result of the bead sample sintered by the ASRTC 1 is

only 1190 HV, and the bead sample sintered by the ASRTC2 is 1210 HV. Both of them are lower than that of beads prepared with the normal sintering rising-time temperature curve. However, if the sintering temperature too high or the holding time too long, the grains will grow abnormally, and the hardness of the beads will also decrease greatly. When using the ASRTC 3, the surface of the sintered beads is shown in Figure 6c, many grains grow abnormally, and the average hardness tested result of bead sample is only 1180 HV, also lower than that of beads prepared with the normal sintering rising-time temperature curve.

### 3.3. SEM and grain tests

#### 3.3.1. SEM tests

The results are shown in Figures 8-13. The main discussions are as follows: 1) From Figure 8a-11a, it can be seen that, each of the prepared bead sizes is accurately controlled, and has good spherical type. 2) Figure 8b-11b show that each of the bead surface grains is compact, and has

no obvious pores and defects among the grains. 3) In order to observe the internal morphology of the beads, the 0.3 mm beads were broken, as shown in Figure 12. The cross section morphologies of the beads are shown in the Figure 11. The defects and pores also not appear among the grains. 4) In order to further accurately test the interior of the beads, the 0.3 mm bead sample block after hardness test in section 3.2 were used. They were eliminated the scratches on the surface with large mesh sandpaper, and characterized by SEM. The result is shown in Figure 13. From the result, it can be got that, the interior of the bead is completely consistent, and has no pores and defects. This method is an innovative method to evaluate the internal structure of beads. Very few beads can achieve this effect with no pores and defects.

The surface and fracture surface morphology SEM images show that there are good consistency between the surface and interior of the beads. This further explains that the new sol-gel titration process method can prepared the beads with high compactness.

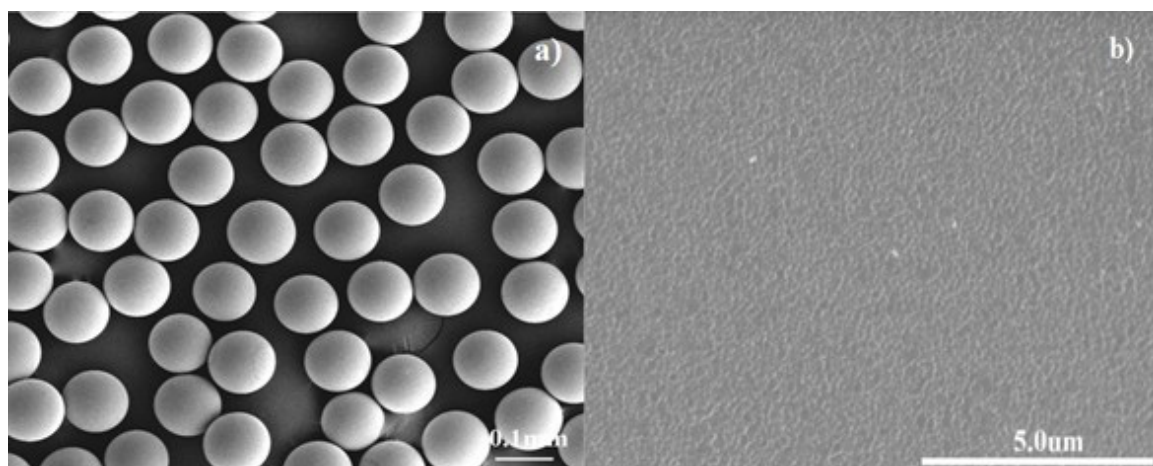


**Figure 8.** The SEM images of the surface morphology of 0.1 mm beads: (a) Low magnification. (b) High magnification.

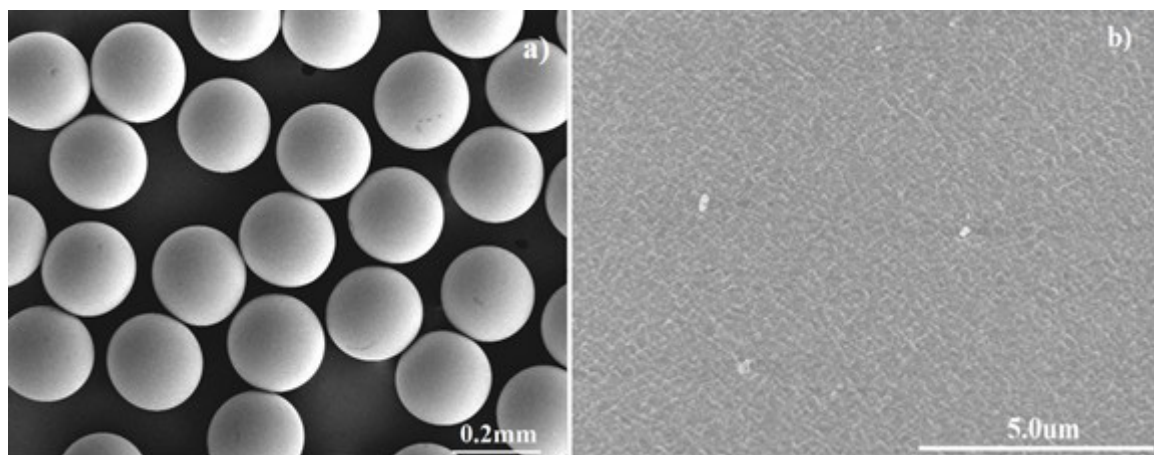


**Figure 9.** The SEM images of the surface morphology of 0.2 mm beads: (a) Low magnification. (b) High magnification.

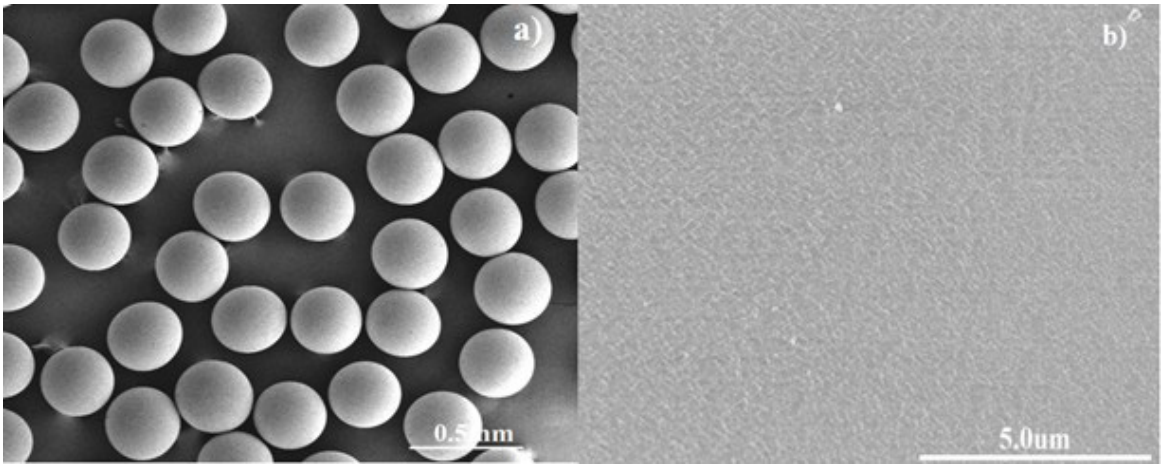


**Figure 10.** The SEM images of the surface morphology of 0.3 mm beads: (a) Low magnification. (b) High magnification.

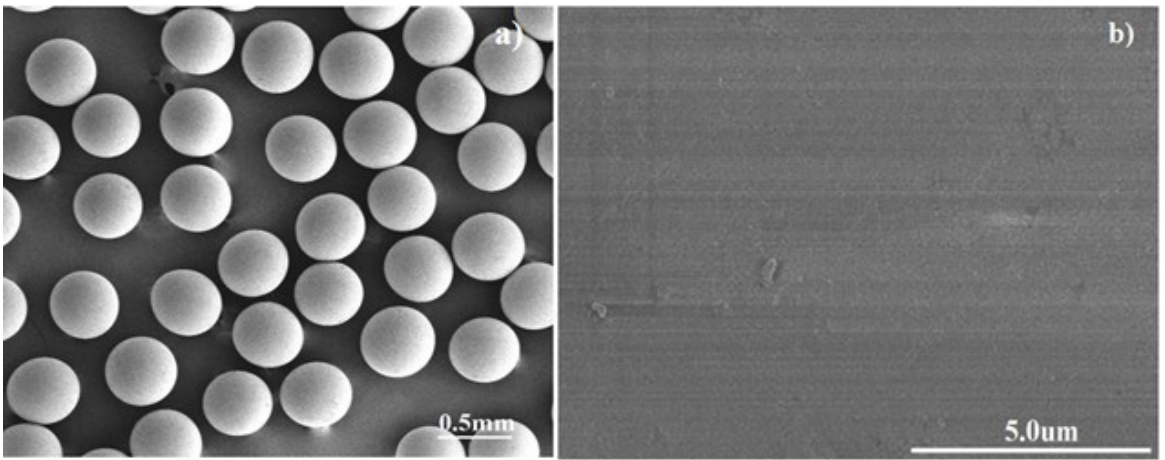


**Figure 11.** The SEM images of the surface morphology of 0.5 mm beads: (a) Low magnification. (b) High magnification.

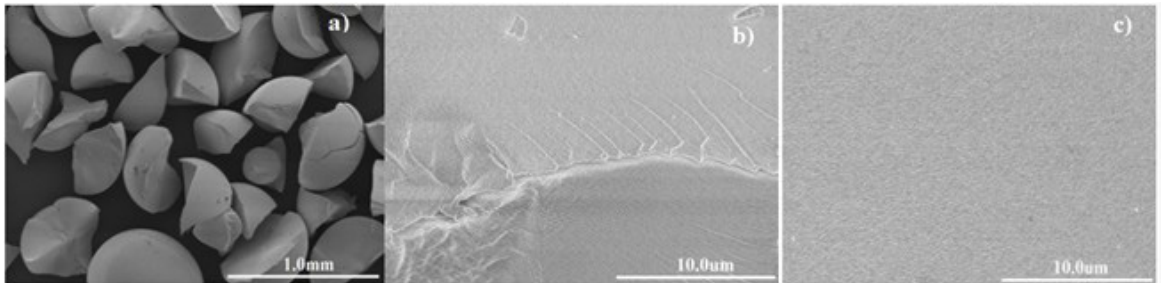


**Figure 12.** The SEM images of the morphology of broken beads: (a) Low magnification. (b) and (c) Cross section under high magnification.

### 3.3.2. The grain test of the beads

In order to explore the grain size of the sintered beads, the grain size of 0.1 mm beads and 0.3 mm beads were measured using the measurement software, the results are shown in Figure 14a and 14b and Tables 4 and 5. To make comparison, the grain size of the 0.3 mm beads prepared by the ASRTC 3 were also tested (abbreviated as Abnormal Beads in subsequent sections). The results are shown in Figure 14c and Tables 4 and 5.

From the Figures 14a and 14b, it can be got that the grains of the beads are compactly distributed, no pores and defects exist among the grains. The reason is that the process is based on the sol-gel technology, each of the bead components is fully reacted in the form of ions and can evenly distribute.

From the Tables 4 and 5, it can be got that the average grain size of 0.1 mm beads tested result is 127.3 nm, and the 0.3 mm beads is 129.7 nm. Both of them are relatively

**Table 4.** The grain size distribution of 0.1 mm, 0.3 mm beads sintered by the normal sintering temperature curve, and 0.3 mm beads sintered by the abnormal sintering temperature curve 3.

Distr./nm	0.1 mm beads	0.3 mm beads	Abnormal beads
	Amount		
0-50	1	1	1
50-100	27	34	34
100-150	39	37	20
150-200	26	21	22
200-250	5	6	19
250-300	2	1	14
>300	0	0	15
Total	100	100	100

**Table 5.** The summary of grain size data of 0.1 mm, 0.3 mm beads sintered by the normal sintering temperature curve, and 0.3 mm beads sintered by the abnormal sintering temperature curve. 3.

Item	0.1 mm beads	0.3 mm beads	Abnormal beads
Max./nm	302.7	271.6	430.7
Min./nm	44.7	49.6	45.7
Mean/nm	127.3	129.7	203.2

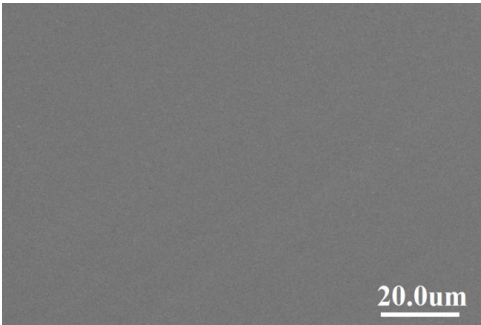


**Figure 13.** The SEM images of the polished cross section morphology of 0.3 mm beads.

close, and the sizes are concentratively distributed on the value of 50 - 200 nm. However, the average grain size of the beads tested result prepared by the abnormal sintering rising-time temperature curve 3 is 203.4 nm, as shown in Tables 4 and 5, and the values range from 50 to 400 nm. The concentration level of the value is greatly inferior to the two kinds of beads mentioned before. This implies that: 1) The average grain size of the beads prepared by the novel method is much smaller than that of the beads prepared by the conventional process which was about 400 nm<sup>9,14-16</sup>. 2) The grain size of the beads is mainly decided by the sol-gel process and the sintering rising-time temperature curve, and has nothing to do with the bead size.

From the tested results of the bead hardness discussed in section 3.2. The sintering rising-time temperature curve has great influence on the bead hardness. The reason is that the sintering rising-time temperature can influence the bead grains growth. If the sintering temperature too low, the bead growth is not completely, and the hardness will be decreased. If the sintering temperature too high or the holding time too long, the grains will grow abnormally, as shown in Figure 14c, which will also cause the hardness decreased. Therefore, it is important to control the grain size through the appropriate sintering rising-time temperature curve which is discussed in section 2.3.2.

3.4. XRD analysis

Figure 15a-d show the XRD patterns of the bead samples. In order to investigate the properties of powder with the same sol-gel process, the powder sample was also tested, and the result is shown in Figure 15e. The sintering temperature for these five samples is 1250°C. The composition of the powder sample is identical with bead samples. For the powder sample preparation, the same sol was used, and the process steps were identical with the beads preparation except without the titration step. The X-ray fluorescence analysis was conducted on five samples, and the content of yttrium

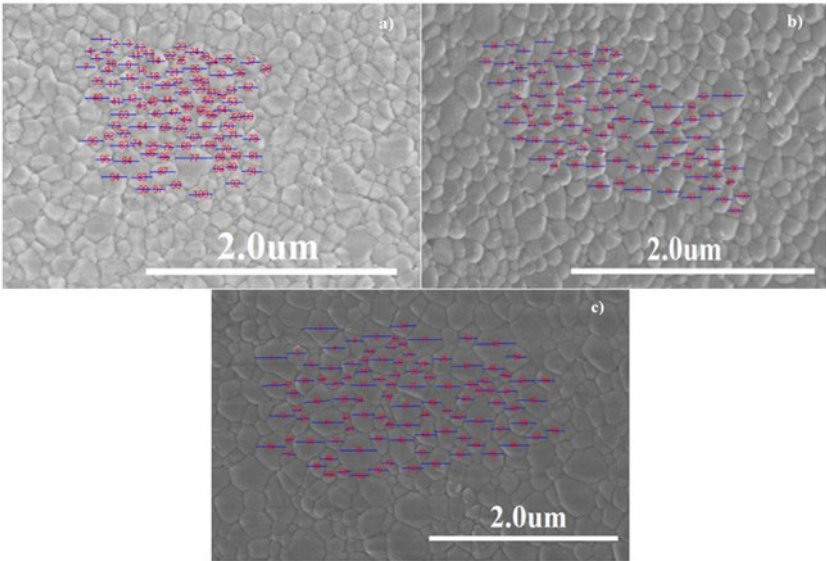


**Figure 14.** The SEM images of grain size test: (a) 0.1 mm beads sintered by the normal sintering temperature curve. (b) 0.3 mm beads sintered by the normal sintering temperature curve. (c) 0.3 mm beads sintered by the abnormal sintering temperature curve 3.

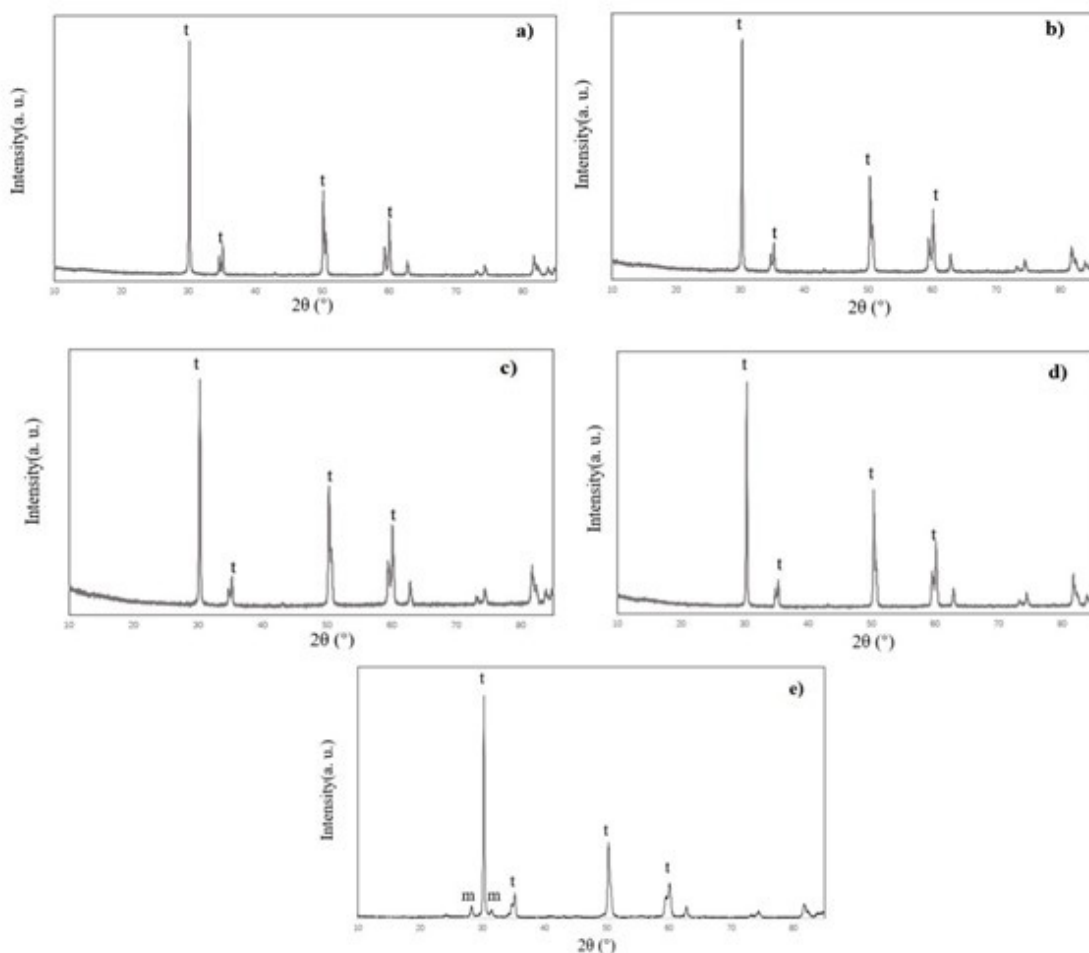


**Figure 15.** The XRD pattern of the (a) 0.1mm beads, (b) 0.2mm beads, (c) 0.3mm beads, (d) 0.5mm beads, and (e) powder sample (m-monoclinic zirconia, t-tetragonal zirconia).

oxide was 5.203%, 5.216%, 5.212%, 5.209%, and 5.211%, respectively. The content of yttrium oxide is relatively close.

The  $2\theta$  angles corresponding to the three strong peaks of tetragonal phase are  $30.2^\circ$ ,  $49.8^\circ$ ,  $59.6^\circ$ , and the  $2\theta$  angles corresponding to the two weak peaks of monoclinic phase are  $28.2^\circ$ ,  $31.6^\circ$ . From the Figure 15, it can be got that: 1) There is no monoclinic phase in the four sample beads before and after  $30^\circ$ , but there are two small peaks in powder at  $28.2^\circ$  and  $31.6^\circ$ , which are monoclinic phase<sup>1,17-20</sup>. The monoclinic phase peaks have been marked in Figure 15e. 2) The same components, and the same sol, through the new sol-gel titration process monoclinic phase in beads can convert to tetragonal phase after sintered at  $1250^\circ\text{C}$ , which fully demonstrates the advanced nature of the wet titration process<sup>21</sup>.

#### 4. Conclusion

In this report, based on the sol-gel titration technology, a novel process method to prepare the ZrO<sub>2</sub> beads with the advantages of 130 nm grains and no pores has been proposed. These advantages can greatly improve the bead density and hardness, decline the sintering temperature. Furthermore,

using the method, the beads of different diameters which range from 0.1 mm to 0.8 mm can be prepared with uniform size and well spherical type. The process steps of the novel method have been shown. The experiments to illustrate the new method have been done. The key influences of the preparation condition have been discussed. The prepared bead density and hardness have been tested, and their morphologies and crystal phase have been characterized and discussed. The tested density results concentrate on  $6.04\text{ g/cm}^3$  and the hardness results on 1280 HV, both of them are higher than that of traditional rolling beads. The optical microscope tests exhibit that the beads after titrated, glue discharged at  $550^\circ\text{C}$  and sintered at  $1250^\circ\text{C}$  are bright and almost transparent, indicating that the surface of the beads is smooth, and the surface and interior of the beads have few pores and defects. The SEM results illustrate that the grains are evenly distributed, and no abnormally grains grow. The average grain size is 130 nm, much smaller than 400 nm that of the ZrO<sub>2</sub> beads prepared by the conventional process, and much smaller than that of the abnormal beads prepared with the abnormal sintered curves. The microscopic morphologies of the bead surface and cross section are approximately

consistent, and no pores existed among the grains of finely polished section. The XRD results demonstrate that no monoclinic phase exists in the beads after sintered. The sintering temperature of the new proposed process method is only 1250 °C, and without insulation, much lower than that of the routine process.

## 5. Reference

1. Wang MT, Chang CP. Development and application of ZrO<sub>2</sub> basen nono composite ceramics. *Chin Ceram*. 2008;44(6).
2. Gan XX, Song XM, Liu N, Dai HY. Effects of grinding equipment and technological parameters on particle size of zirconia powder. *Refractories* 2018;52(3):205-08.
3. Noh Y, Lee YJ, Kim J, Kim YK. Enhanced efficiency in CO<sub>2</sub>-free hydrogen production from methane in a molten liquid alloy bubble column reactor with zirconia beads. *Chem Eng J*. 2022;428:131095.
4. Liu S, Tokura R, Thanh NM, Tsukamoto H, Yonezawa T. Surfactant-stabilized copper paticles for low-temperature sintering: Paste preparation using a milling with small zirconia beads: effect of pre-treatment with the disperse medium. *Adv Powder Technol*. 2020;31(11):4570-75.
5. Komatsu T, Ohta H, Motegi H, Hata JC, Terawaki K, Koizumi M, et al. A novel model of ischemia in rats with middle cerebral artery occlusion using a microcatheter and zirconia ball under fluoroscopy. *Sci Rep*. 2021;11(1):12806.
6. Motoyoshi K, Hiroko N, Yoshiko M. Initial deposition rate of latex particles in the packed bed of zirconia beads. *Colloids Surf A Physicochem Eng Asp*. 2008;347(1-3):2-7.
7. Song DH, Kim JY, Kahng YH, Cho H, Kim ES. Long-term effects on graphene supercapacitors of using a zirconia bowl and zirconia balls for ball-mill mixing of active materials. *J Korean Phys Soc*. 2018;72(8):900-05.
8. Jia GY, Zhang WR, Fan JL. Development of low cost zirconia grinding balls, [J]. *Material Guide* 2000;14:74-75.
9. Lv BW. The preparation and study of ZrO<sub>2</sub> grinding media ball. Shandong: Shandong University of Technology; 2008.
10. Walter M, Somers J, Fernandez A, Specht ED. Structure of yttria stabilized zirconia beads produced by gel supported precipitation. *J Mater Sci*. 2007;42(12):4650-58.
11. Guo T, Wang C, Dong LM, Lu JL, Liang TX. Effect of Al<sub>2</sub>O<sub>3</sub> on the process performance of ZrO<sub>2</sub> microspheres. *J Wuhan Univ Technol*. 2020;35(5):841-46.
12. Liu JL, Ma ZA, Pan JC, Wang CM. Study on preparation of millimeter-sized alumina pellets by hot oil-drop method with pseudo-boehmite. *Petroleum Process Petrochem*. 2019;50(5):1-5.
13. Wei LW, Yang DY, Yuan HY, Cui JY, Wang ZF. Effect of polishing time and sintering temperature on properties of alumina balls. *Naihuo Cailiao* 2020;54:493-96.
14. Liu W, Zhang HJ, Zhang WH. Study on preparation technique and properties of zirconia wear resistant ceramic beads manufactured by a roll-forming method. *Rare Met Mater Eng*. 2009;38:198-01.
15. Ji YM. Study on roll-forming technology and performance of ZrO<sub>2</sub> ceramic microbeads. Inner Mongolia: Inner Mongolia University of Science and Technology; 2020.
16. Li YF, Zhou ZW, Wang ZH. Effect of speed sintering system on mechanical properties od zirconia. *Stomatol Res*. 2021;37(4):339-43.
17. Garvie RC. The occurrence of metastable tetragonal zirconia as a crystallite size effect. *J Phys Chem*. 1965;69:1238-43.
18. Wang JF, Zhang GH, Zhou GZ. Preparation of nanocrystalline zirconium dioxide powder. *Jiangxi Metall*. 2011;40(3).
19. Xu HL, Lu HX, Wang HL, Chen DL, Zhang R. Preparation of tetragonal zirconia's powder. *Chin Ceram*. 2008;44(6).
20. Yi ZZ, Shan K, Zhai FR, Li N, Xie ZP. Structure and properties of thermal barrier coating prepared by alumina coated zirconia composite powder. *J Chin Ceram Soc*. 2018;46(3):328-32.
21. Lv BV, Yan FQ, Chen DM. Effect of sintering temperature on peoperties of zirconia wear resistant ceramic ball. *J Adv Ceram*. 2007;4:3-5.